Royal Norwegian Council
for Scientific and Industrial Research
(NTNF)

NORSAR

NORSAR Scientific Report No. 1-88/89

Final Technical Summary

1 April – 30 September 1988

L.B. Loughran (ed.)

Kjeller, December 1988

VII.3 Modelling of Lg-wave propagation across the Central Graben of the North Sea

This is the third and final report on modelling of Lg wave propagation in the Central Graben of the North Sea in an attempt to explain the very strong attenuation of the Lg wavetrain observed in this area. In the first report (Maupin, 1987), we presented the modelling method and some preliminary tests. The bulk of the modelling results, i.e., the reflection and transmission matrices for Rayleigh and Love type Lg-modes propagating at a right angle or at an oblique angle across a graben model, were presented in the second report (Maupin, 1988). A first interpretation of the matrices showed that on the average over many Lg wavetrains, 80% of the incoming Lg energy remains in the Lg wave after propagation across the graben model.

The transmission matrix affects differently incoming Lg wavetrains with different modal contents. The relative amplitudes of the different modes, which depend on their excitation by the seismic source, as well as their phase differences when reaching the Graben, which vary with epicentral distance, define the modal content. In order to exploit more completely the transmission matrix, we analyze here its effect on Lg wavetrains from different sources at different distances from the Graben. Since the transmission of Rayleigh and Love waves at a right angle or at an oblique angle across the model have been found very similar in the second report, we concentrate our analysis here to Rayleigh waves propagating at right angles across the structure. On the other hand, the transmission across three variants of the Central Graben model used in the previous reports (and now called model 1) are also examined, to account for possible block-faulting of the Graben margin (models 2 and 3, Fig. VII.3.1) or roughness of the sediment-basement interface (model 4, Fig. VII.3.1). We also examine the phase stability with period of the transmitted wavetrain.

After inspection of the results for different sources, we retain three typical cases for discussion: an explosion, a strike-slip earthquake with a fault trace at 75^{o} from the symmetry direction of the Graben,

and an earthquake which occurred on the western flank of the Viking Graben on 29 July 1982 (strike: 100°, dip: 63°, slip: -170°, after Havskov and Bungum, 1987), for which we study the waves travelling due east perpendicularly across the Viking Graben and to Norway. We use explosions with 4 different focal depths, ranging from 0 to 3 km, and earthquakes at 7 different focal depths sampling the whole crust. The distances of the events from the Graben are taken ranging from 0 to 1000 km, with a step of 10 km, providing a good sampling of possible phase shifts between the different modes when reaching the Graben. These events do not intend to model a complete or realistic situation, but to provide an oversight of the effect of the Graben on different Lg wavetrains. We recall that Gregersen (1984) used many earthquakes in his study of the attenuation across the North Sea Central Graben, and pointed out that the effect does not depend on the source.

The total energy transmission

For each source type, depth and distance, we calculate the amount of total energy contained in the Lg wavetrain before and after propagation across the Graben. This total energy includes the energy contained in the whole crust for the 11 Lg modes. For each source mechanism and depth, the results are summarized in a histogram of the transmission ratios, which illustrates how their values vary for different source-graben distances.

One of these histograms is shown on Fig. VII.3.2. It displays the values of the transmission ratios across model 1 for an Lg wavetrain excited by a Viking Graben earthquake at 15 km focal depth. The distribution is well peaked around transmission ratios of 80%. Histograms for other focal depths, source mechanisms or models are very similar in shape, with a slight shift of -10% for explosions close to the surface. Fig. VII.3.3, where incident and mean transmitted energies are plotted as a function of source type and depth, also testifies that in the large majority of cases, 80% of the incident energy is transmitted as an Lg wave across our models of the Central Graben. The remaining 20% is converted to Sn or other S waves propagating in the mantle.

This result is in agreement with the findings in report no. 2, and shows that the total energy transmission ratio is only slightly dependent on the source mechanism which has excited the Lg wavetrain.

The surface energy transmission

Since surface waves have their energy distributed with depth differently from one mode to the other, their total energy does not directly indicate how much of the energy is confined close to the surface, or equivalently the surface displacement. More in agreement with what can actually be measured, we therefore also analyze the ratios of transmitted over incident surface energy. This surface energy is the energy of the whole Lg wavetrain measured on the vertical component of a seismometer. The ratios of transmitted over incident maximum vertical displacement at the surface were also calculated, but are not discussed here since the more global character of the energy makes it *a priori* a more stable quantity for estimating the attenuation. We do, however, observe a high degree of similarity between the ratios in energy and in maximum displacement.

The pattern of surface energy transmission is very different from the pattern of total energy transmission. Three typical histograms of surface energy transmission ratios for different source-graben distances are displayed on Fig. VII.3.4, and incident and mean transmitted surface energies as a function of source depth are plotted in Fig. VII.3.5 and VII.3.6 for different sources. In order to indicate the dispersion in the transmission due to changes in the models, we plot the maximum and minimum values of the mean transmitted energies calculated with models 1 to 4. No rule applies as to which model usually gives the lower or higher value.

Fig. VII.3.4a is a typical histogram for explosions or very shallow earthquakes, for which the surface transmission ratios are smaller than the total energy transmission ratios. For these sources, a large part of the total Lg energy is confined close to the surface of the model, mainly in the sedimentary layer, before reaching the Graben. Crossing

the Graben shifts part of the energy deeper in the crust by redistributing the energy more evenly among the different Lg modes. This effect amplifies at the surface the global loss of Lg energy. The surface signature of the Lg wave is therefore decreased by a factor of 0.6 to 0.75 in terms of mean amplitude of the signal.

Some earthquakes with certain focal mechanisms or located at the bottom of the crust excite more evenly the different modes of the Lg waves. This is the case for mid-crustal or deep strike-slip earthquakes, for example, which have rather well-peaked transmission ratio distributions (Fig. VII.3.4b), similar to those for the total energy, and mean values of surface energy transmission around 80% (Fig. VII.3.5). In that case, the mean surface displacement is decreased by a factor of 0.9 after crossing the Graben, and this directly accounts for the total loss of energy in the Lg wavetrain.

Other types of mid-crustal earthquakes, like the mid-crustal Viking Graben earthquake, excite primarily the Lg modes having their energy confined in the middle of the crust. The surface energy before reaching the Graben is thus small compared to the total energy involved in the Lg wavetrain. By crossing the Graben, the energy is redistributed among the modes, and some energy is thereby shifted from the middle of the crust towards the sedimentary layer and the surface. The net effect is an increase in surface energy (Figs. VII.3.4c and VII.3.5), despite the decrease of total energy. In that case, an increase of 1.4 can be expected for the mean amplitude of the recorded Lg wavetrain.

The total energy transmission ratios have shown that the Moho remains a rather energy-proof barrier (only 20% of the energy leaks into the mantle). On the other hand, the surface energy ratios show that the crustal thinning of the Central Graben causes important transfers of energy among the different units of the crust. Comparing the surface energy curves (Figs. VII.3.5 and VII.3.6) with the total energy ones (Fig. VII.3.3), we see that the surface energy curves are very different from the total energy ones before propagation across the Graben (filled symbols), but much more similar afterwards (open

symbols). The Graben has redistributed more evenly within the crust the total energy involved in the Lg wavetrain, and the surface energy reflects better the total amount of energy contained in the whole crust.

Propagation across our Graben models leads to some Lg amplitude variations at the surface, though limited in size and both positive and negative. They are very different from the factor 0.25 to 0.5 actually observed in the North Sea Graben area. Moreover, the preferred focal depth of seismic events in the North Sea is very often around 15 km (Havskov and Bungum, 1987), which would bias our transmission ratios towards their highest values. Our modelling would at the most explain a factor of 2 between the attenuation of Lg waves produced by explosions and Lg waves produced by earthquakes, but can in no case explain the general and strong attenuation observed in this area.

Coherency of the phase with period

The previous calculations have been made at a single frequency. The phase behavior of the waves as a function of period is a key element to the effective build-up of a wavetrain. If rapid variations are observed, interferences between neighboring periods might destroy the wavetrain. In order to check the stability of the phase as a function of period, we now compare the phases of the Lg wave modes propagating out of the Central Graben at 2 neighboring periods, 1.0 and 1.02 s.

We calculate the transmission matrices at the 2 periods. For the same series of sources and source-graben distances as earlier in this report, we calculate the phase of each Lg mode propagating out of the Graben at the 2 periods. We must note that a mode propagating out of the Graben originates from the combination in the Graben of different modes initially excited by the source. Its phase thus depends in a complicated way on the phases of these modes when they enter the structure. We subtract from the total phase the pure propagation phase, i.e., the integral over horizontal distance of the mode local phase slowness. By using a phase free of pure propagation effect, the phase difference between the modes at the 2 different periods is actually

measured at the arrival time of the mode predicted by its group velocity.

On Fig. VII.3.7 are displayed three histograms of the phase differences for the different modes and different source-graben distances after propagation across model 1. Due to the unknown but certainly poor accuracy of the transmission matrix phase, which is influenced by the zoning of the model, we cannot use these histograms very quantitatively. Even if in the second one large phase differences occur rather frequently, cases a) and c) testify that the phases of the modes are not systematically random after crossing the Graben, and therefore cannot give rise to a generally strong attenuation of the wavetrain by destructive interference.

Conclusion

The investigations presented in this report confirm the conlusions already drawn in the second report.

Our numerical modelling of Lg wave propagation in a simplified model of the North Sea Central Graben does not predict the severe attenuation of the wavetrain actually observed in this region. On the contrary, the Lg wavetrain appears very robust when crossing a zone where its waveguide is strongly deformed.

Since the large-scale geometry of the Graben fails to explain the observed data, we suggest that future work explore alternative explanations for the observed attenuation. Scattering by 2D or 3D basaltic intrusions in the lower crust, extensive faulting associated with intra-fault weak material, or more rheological aspects might be good candidates.

V. Maupin, Postdoctorate Fellow

References

Gregersen, S. (1984): Lg-wave propagation and crustal structure differences near Denmark and the North Sea. Geophys. J.R. astr. Soc., 79, 217-234.

Havskov, J. and H. Bungum (1987): Source parameters for earthquakes in the Northern North Sea. Norsk Geol. Tidsskr., 67, 51-58.

Maupin, V. (1987): Preliminary tests for surface waves in 2-D structures. NORSAR Semiann. Tech. Summ. 1 Apr - 30 Sep 1987, NORSAR, Kjeller, Norway.

Maupin, V. (1988): Coupling of short period surface wavetrains across the North Sea Graben, NORSAR Semiann. Tech. Summ. 1 Oct 1987 - 31 Mar 1988, NORSAR, Kjeller, Norway.

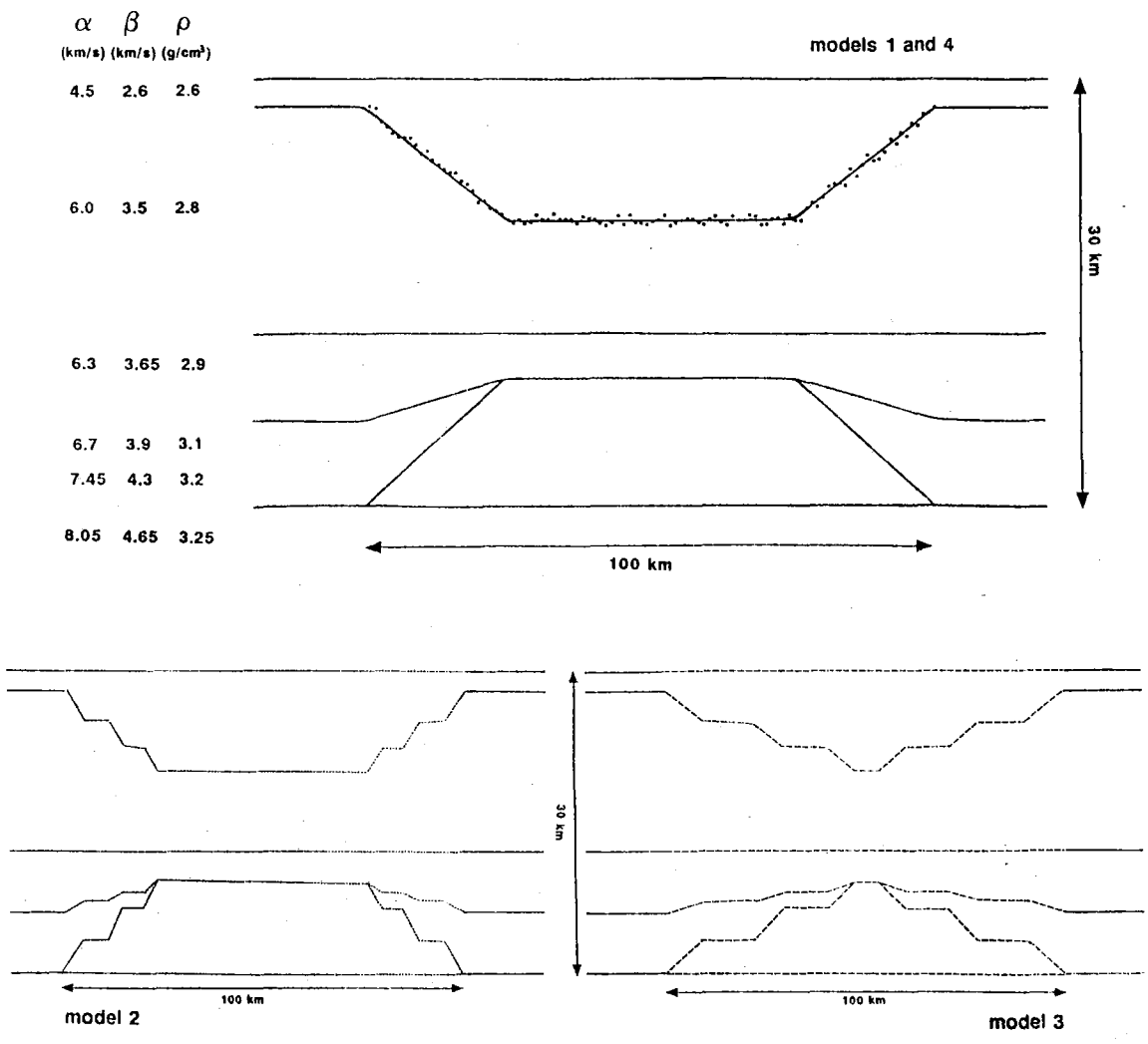

Fig. VII.3.1. Models of the North Sea Central Graben.

Model 1: Full line model, used in the previous reports
Models 2 and 3: Block-faulted models
Model 4: The same as Model 1 with perturbations of the sediment-basement interface represented by a dotted line.

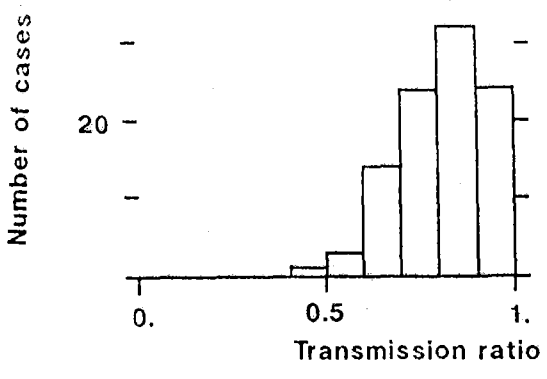

Fig. VII.3.2. Histogram of the energy transmission ratios for a Viking Graben-type event at 15 km focal depth and distances from the Graben ranging from 0 to 1000 km.

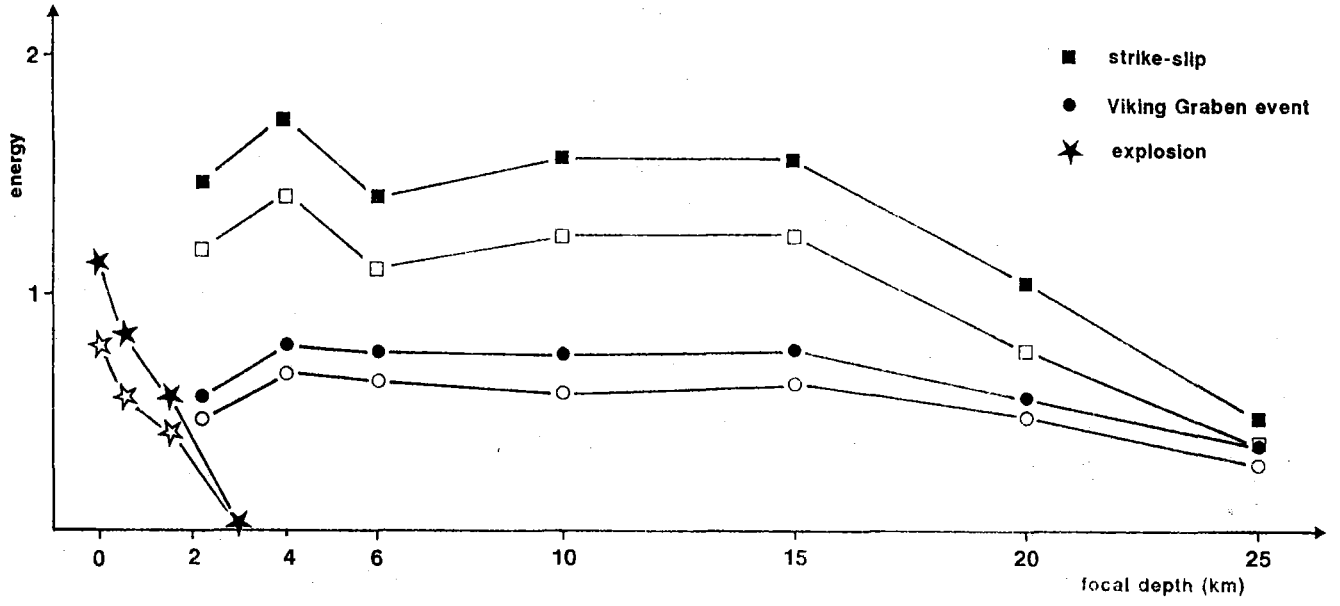

Fig. VII.3.3. Total energy in the Lg wave before (filled symbol) and after propagation across model 1 (open symbol), as a function of source type and depth. The energy scale is only relative since no physical source size is included in the modelling.

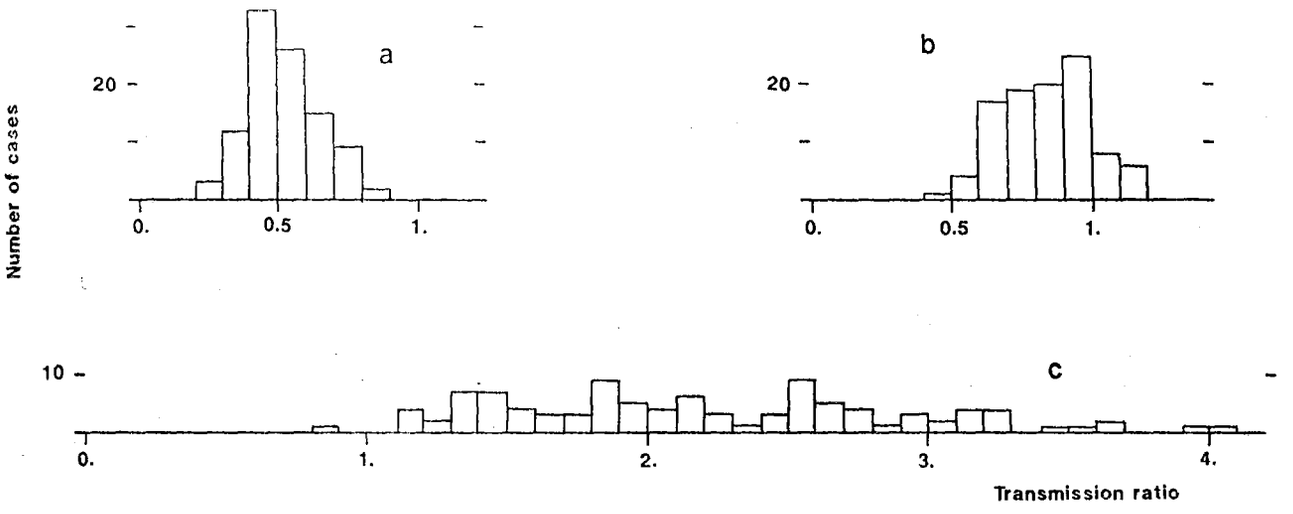

Fig. VII.3.4. Histogram of surface energy transmission ratios for: a) an explosion at the surface; b) a strike-slip event at 15 km focal depth; and c) a Viking Graben-type event at 15 km focal depth and, for all cases, distances from the Graben ranging from 0 to 1000 km.

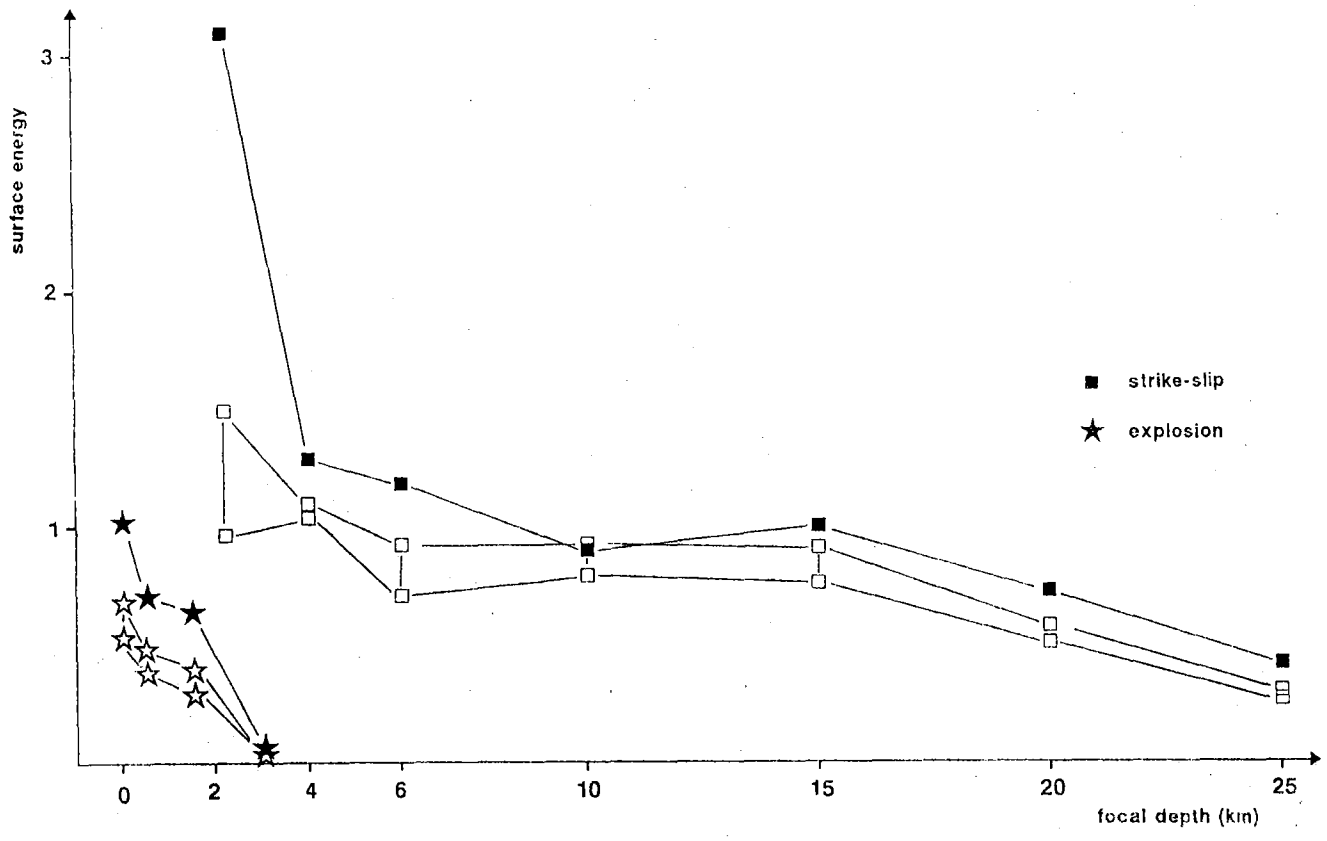

Fig. VII.3.5. Surface energy in the Lg wave measured on the vertical component before (filled symbol) and after propagation across the Central Graben (open symbol), as a function of source type and depth. The minimum and maximum values of transmitted surface energies averaged over different source-graben distances for the four Graben models are represented. The energy scale is only relative since no physical source size is included in the modelling.

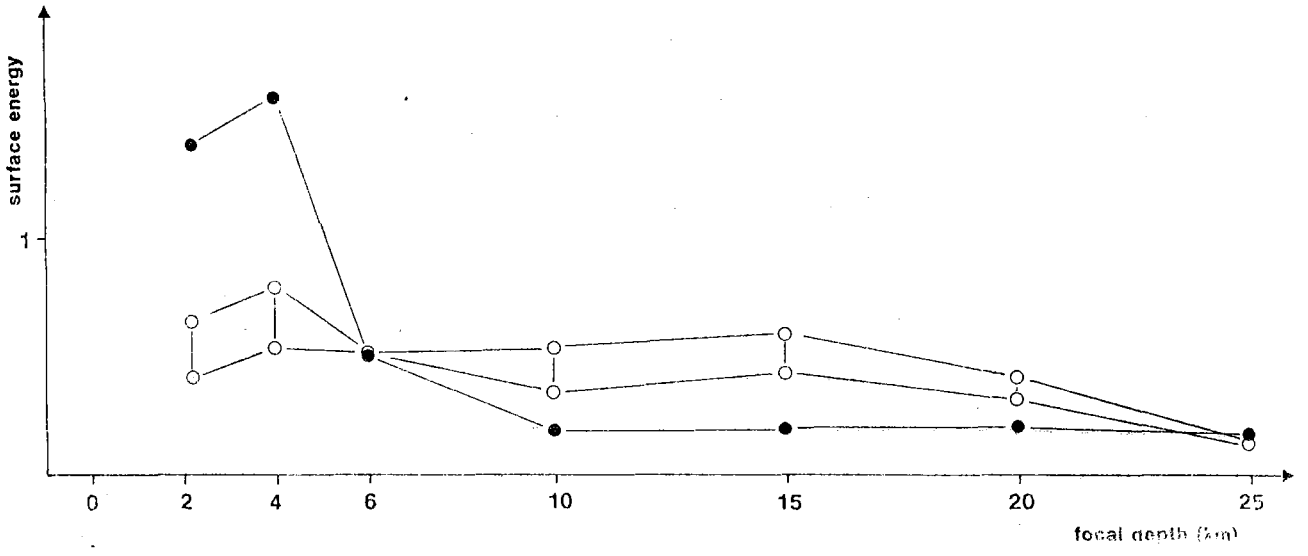

Fig. VII.3.6. The same as Fig. VII.3.5 for Viking Graben-type events.

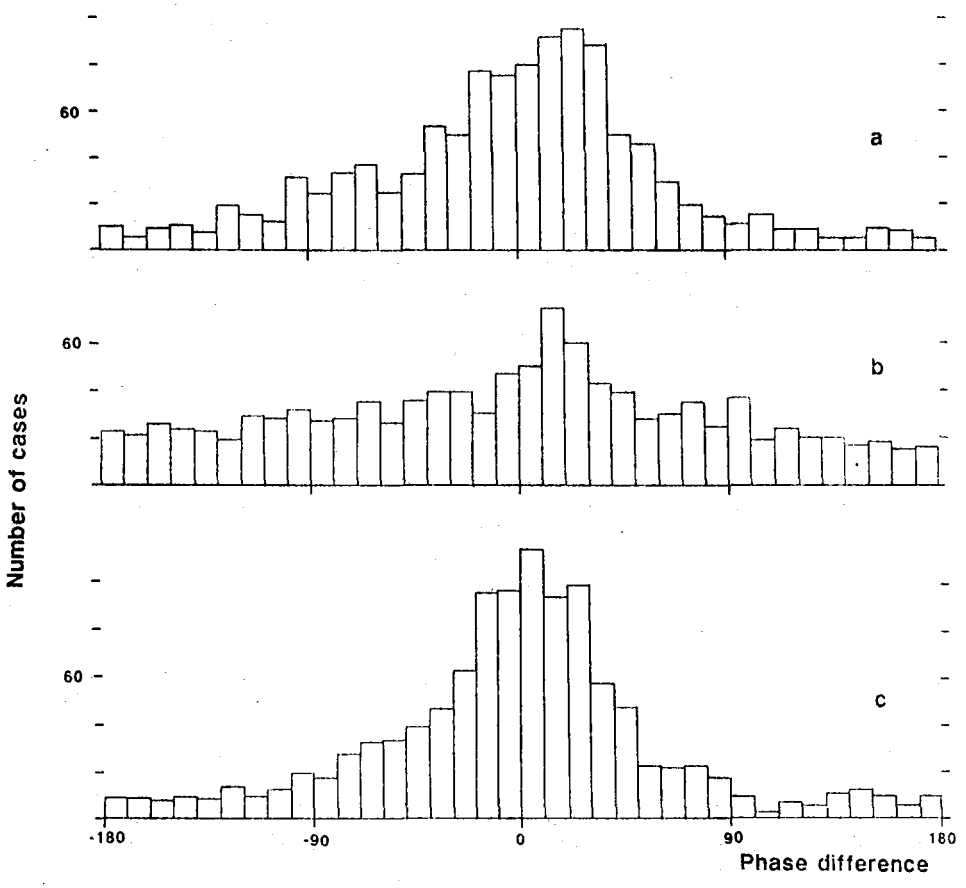

Fig. VII.3.7. Histogram of the phase difference between Lg modes at periods 1.0 and 1.02 s after propagation across model 1, for: a) an explosion at the surface; b) a Viking Graben-type event at 2.2 km focal depth; and c) a Viking Graben-type event at 15 km focal depth, and, in all cases, distances from the graben ranging from 0 to 1000 km.